

Ballistic-electron-emission microscopy of semiconductor heterostructures

L. Douglas Bell
MIS 302-231
Jet Propulsion Laboratory
Pasadena, CA 91109 USA
Tel: 818-354-4761
FAX: 818-393-4540
email: dbell@vaxeb.jpl.nasa.gov

Venkatesh Narayanamurti
Dean, College of Engineering
University of California
Santa Barbara, CA 93106 USA
Tel: 805-893-3141
FAX: 805-
email: venky@ec11.ucsb.edu

Summary

Ballistic-electron-emission microscopy has developed from its beginning as a probe of Schottky barriers into a **powerful** nanometer-scale method for characterizing semiconductor interfaces and hot-electron transport. Recent applications include band offsets, electron scattering, confined states, interracial defects, and insulating layers.

Introduction

Over the last 15 years scanning tunneling microscopy (STM) has made an immense contribution to an understanding of surfaces on an atomic scale [1]. The field has also spawned a general interest in local probe methods, an acknowledgment of the unique strengths and capabilities of these techniques. Ballistic-electron-emission microscopy [2,3,4] (BEEM) extends the reach of STM to subsurface semiconductor interfaces and hot-electron transport. Several reviews of earlier work have appeared previously [5,6]. More recently, its areas of utilization have multiplied, with many promising applications still to be explored.

In STM a voltage is applied across the tunnel gap between probe tip and sample, and a measurement is made of tunnel current at constant tip height (spectroscopy) or tip height at constant tunnel current (topographic imaging). Information is obtained about the sample which reflects surface or near-surface structure, since only near-surface properties affect the tunneling characteristics. In contrast, BEEM is a three terminal measurement; a second sample contact measures the fraction of the tunnel current which traverses the sample and enters the collector layer. Figure 1 illustrates the BEEM configuration. STM normally operates in feedback mode at constant tunnel current; thus, BEEM spectra are normalized to constant injected current. This type of normalized spectrum greatly enhances the ability to distinguish spectral features, as well as reducing variation which is due only to varying surface properties.

BEEM takes full advantage of the atomic-scale imaging capability of STM. The very high spatial resolution (atomic-scale) of STM translates to high spatial resolution (nanometer-scale) of subsurface properties. In the presence of interface heterogeneity, this high resolution allows isolated characterization of nanometer-scale areas with different electronic structure. In contrast, macroscopic probing with other techniques yields a weighted spatial average of interface properties.

BEEM represents a significant advance over conventional interface characterization in several other respects. Electronic structure may be probed over a wide energy range about the Fermi level (0-- 10 eV) by precise control of injected electron energy, simply by varying the voltage applied to the STM tip. Interface characterization by conventional methods, such as current-voltage or capacitance-voltage measurement, is restricted to probing with low-energy (near-equilibrium) electrons. A further advantage of BEEM is that no voltage is required across the sample structure itself, allowing investigation of interface structure which is unperturbed by voltage-induced band bending. Finally, since BEEM is a well-controlled carrier transport spectroscopy, BEEM spectra and images are sensitive to other aspects of transport such as scattering processes.

BEEM was first applied to metal/semiconductor (M/S) Schottky barrier interfaces [2,3]. Schottky barrier heights were determined with high precision, and direct imaging of interface heterogeneity was accomplished. Features due to higher-energy interface structure (conduction-band minima) were observed in BEEM spectra, and the first hole spectroscopy using BEEM techniques was performed [7]. These early experiments also yielded a direct measure of hot-electron mean-free path in Au [8].

Metal/semiconductor interface properties

The first area of application of BEEM has continued to be of great interest. Schottky barrier interfaces are **fundamental** to many classes of devices, and shrinking device dimensions have produced renewed interest in interface uniformity. Following much work on Si- and GaAs-based systems, other materials have more recently been studied by BEEM techniques.

ZnSe is one material for which reports of Schottky barrier height have differed widely. As in most cases, variations in chemical treatment and surface stoichiometry are thought to be responsible. Morgan et al. [9] have investigated barrier heights for Au/ZnSe contacts. Interestingly, they found different mean barrier heights and narrower height distributions than in previous results by Coratger et al. [10] This was attributed to a difference in surface preparation and stoichiometry. Further work [11] compared these barrier height variations with those of PtSi/Si. The wider variation in barrier height observed for Au/ZnSe was attributed to rough interface topography. Dharmadasa et al. [12] and Coratger et al. [13] reported a range of discrete barrier values for metal/ZnSe ranging from 0.90 to 2.10 eV, a unified series of values which is independent of metal species. This is correlated with the existence of multiple pinning positions. Presumably the local predominance of one type of defect over others, or local variations in stoichiometry, might determine which pinning position and barrier height occurs.

In a comparative study of Au Schottky contacts on several semiconductors by Morgan et al. [14], variations of barrier height were generally observed to increase for compound semiconductors and for higher substrate doping. A reduction in the effect of field pinch-off is proposed as a likely explanation for the latter effect.

The investigation of the atomic-scale nature of defects at interfaces is an area where BEEM has unique advantages. Siringhaus et al. [15**] have imaged individual point defects at the CoSi₂/Si(111) interface, which were observed due to their effect on electron scattering. A lower Schottky barrier was observed at defects for (1 00) interfaces, whereas it was absent for the(111) orientation. Meyer and von Känel [16**] continued this work, observing that these point defects accumulate at dislocation cores. A pair of images illustrating this observation is given in Fig. 2.

Effects due to interface modification have been studied previously in BEEM experiments, due to the importance of understanding the evolution of interfaces in response to temperature or other processing steps. The effect of focused ion beam implantation on BEEM spectra of Au/GaAs was investigated by McNabb and Craighead [17]. Increased scattering due to induced defects was invoked as the cause of reduced transmission in the implanted areas. Sumiya et al. [18] have studied the effects of annealing and high-temperature deposition on BEEM spectra of Au/Si(111). The observed elimination of collected current **after** a 300°C anneal was attributed to Au/Si **interdiffusion** which is known to occur at elevated temperatures.

Novel materials will continue to be a focus of BEEM research. Brazel et al. [19*] performed measurements on the Au/GaN system, where transmission was observed only in a few areas. This most likely resulted from the relatively poor material quality of GaN or from as-yet unidentified interface effects, and emphasizes the unique capabilities of BEEM for the identification of non-**ideal behaviour** in interface transport.

Scattering and transport in metal/semiconductor structures

Hot-electron transport in metals and across the M/S interface has been investigated by BEEM since its inception, but there are many details which are still uncertain. One central issue for which there has been no definitive answer is whether elastic interface scattering plays a strong role in the interface transport process. Recent work has shed some light on this question, but much work remains to be done. **Ventrice** et al. [20*] performed BEEM spectroscopy on Au/Si(100) structures at room temperature and at 77K. By observing the temperature dependence of BEEM current attenuation with Au thickness, they concluded that strong interface scattering was responsible for the results.

A theoretical treatment of transport in the Au/Si system was presented by **Garcia-Vidal** et al. [21]. The similarity of (111) and (100) spectra was described by focusing of electrons along certain trajectories by the Au band structure. Since the (111) orientation is the one expected to show very different **behaviour** in the presence or absence of scattering, **Bell** [22* ,23] performed BEEM spectroscopy on Au/Si(111) as a function of Au thickness and temperature. The surprising feature of these experiments was the appearance of anomalous spectra at 77K for thick Au layers (Fig. 3). This was explained in terms of parallel momentum conservation at the M/S interface, coupled with the contribution of multiple electron passes through thin Au layers. As argued in this model, multiple passes did not have a strong effect with thick Au layers, and at low temperature phonon scattering was reduced, allowing the effects of parallel momentum conservation at the Au/Si interface to be observed. A direct signature of multiple passes was observed in attenuation length measurements at very thin Au coverages. It was pointed out that the appearance of the anomalous spectra only at low temperature argued against a model involving Au band structure.

Guthrie et al. [24**] performed extensive calculations and low-temperature measurements for Au/Si and Au/GaAs, at temperatures down to 7K. Their data and modeling also indicated extensive elastic scattering and suggested multiple electron reflections within the metal layer, but thickness dependence was not discussed.

Semiconductor heterostructures

The uses of BEEM now extend well beyond its initial application to M/S systems. More recently BEEM has been used to probe interfaces and transport in semiconductor heterostructures. **Ke** et al. [25] performed BEEM on Au/GaAs/AlAs samples, Monte Carlo simulations led to the conclusion that transmission across the Au/GaAs interface was incoherent, whereas GaAs/AlAs transmission was coherent. This work was followed by spectroscopy on Au/InAs/GaAs [26], where a lowering in barrier height was observed with increasing InAs thickness. This lowering was explained in terms of a relaxation of the In As layer. Additionally, spectra for InAs layers thicker than two monolayer (ML) showed only two thresholds. Parallel momentum conservation at the InAs/GaAs interlace was argued to account for this observation.

A thorough study of the AlGaAs/GaAs system using BEEM was also reported by O' Shea et al. [27**]. Spectroscopy was performed over the entire Al alloy fraction range, and temperature was

also varied. Certain contributions to collected current were observed to vary strongly with temperature, supporting the argument that phonon-assisted **intervalley** scattering was responsible for these contributions. Measured band positions in the **AlGaAs** layers agreed well with calculations.

A theoretical treatment of BEEM spectroscopy through single- and double-barrier semiconductor **heterostructures** has been presented by Smith and Kogan [28*]. Transmission coefficients were calculated for the **heterostructures** and used within the phase-space framework of the original BEEM model. These calculations yielded reasonable agreement with previously reported experimental results [29] on double-barrier resonant tunneling structures.

Other III-V **heterostructures** have been probed by BEEM. O' Shea et al. [30**] made band-offset measurements on **GaInP/GaAs**. The value of this offset was observed to vary, decreasing with increasing alloy ordering in the **GaInP** layer. By growing on disoriented GaAs substrates, this ordering was enhanced or inhibited. In **BEEM** measurements on **Au/InAs/AlSb** structures, **Bhargava** et al. [31*] measured a single spectral threshold corresponding to the AlSb conduction-band minimum. By comparing this with the **InAs/AlSb** band offset obtained from **capacitance-voltage** measurements, they obtained an estimate of the Fermi level pinning position in InAs.

Imaging of misfit dislocations at the **InGaAs/GaAs**(100) interface was accomplished by Lee et al. [32**]. Surface topographic protrusions resulting from the dislocations were observed in conjunction with diminished **BEEM** current (Fig. 4); however, the two features were laterally displaced relative to each other. This displacement, which demonstrated that the source of the features was subsurface, is expected if the dislocations glide along {111}. Either strain-induced lattice deformation or trapped charge was proposed to explain the measured logarithmic spatial dependence of the BEEM reduction at the dislocations. Initial calculations of expected BEEM resolution for these dislocations [33] agreed well with observed resolutions.

Superlattices, quantum wires, quantum dots

Low-dimensional structures have also recently been the focus of several BEEM efforts. Westwood et al. [34] reported observation of BEEM current modulation due to compositional modulation in buried **GaAs/AlAs** lateral **superlattices**. Eder et al. [35] have utilized lateral patterning of **GaAs/AlGaAs** heterostructures to produce quantum wires. Using BEEM spectroscopy different barrier heights and transmissions were observed over the wires. Further work was **performed** at liquid helium temperature [36] with the additional goal of extracting a precise threshold power law, but the results were inconclusive.

Self-assembled InAs quantum dots were probed by Rubin et al. [37**] using BEEM spectroscopy and imaging. The experiment is schematically shown in Fig. 5. The dots were fabricated on GaAs substrates, and a GaAs capping layer was then deposited. Different behaviour was observed for spectra over the dot areas compared with spectra away from the dots. Band shifts due to strain effects in the GaAs cap were observed, and additional structure was attributed to resonant transport through confined states in the quantum dot.

Whereas InAs quantum dots produce local potential wells when grown on GaAs, GaSb dots produce local potential steps. Rubin et al. [38] also performed spectroscopy and imaging on GaSb dots on GaAs, again with a GaAs cap. STM and BEEM images of a single GaSb dot are shown in Fig. 6. By comparison of on-dot and off-dot spectra the **GaSb/GaAs** band offset was extracted.

Recent Monte Carlo calculations of BEEM transport addressed spatial resolution of this technique for the imaging and spectroscopy of buried quantum dots and wires [39]. Although no comparison of the calculations with experimental data was attempted, it was concluded that similar calculations should allow extraction of electronic structure parameters for buried **low-dimensional** structures.

Oxide properties and MOS structures

Since **Si-based** MOS systems are of such critical importance in current microelectronic device technology, they represent an important class of structures to characterize on the deep **submicron** scale. **Kaczer** and **Pelz** [40*, 41] have applied BEEM to **SiO₂/Si** to investigate the effects of charge trapping in the oxide. Local suppression of **BEEM** transmission was observed in areas which were subjected to electron charging from the STM tip. This suppression was accompanied by an increase in BEEM threshold voltage. These changes were explained by charge-induced band-bending of the **SiO₂** conduction band. Some discussion of the lateral extent and lifetime of the suppressed area was also presented. Recent results by Ludeke and Wen [42] have also addressed the charging of **SiO₂** layers, distinguishing between the effects of **pre-existing** defects and stress-induced traps.

Ludeke et al. [43**] have continued this work on BEEM of **SiO₂** layers. By comparing Monte Carlo calculations to experimental spectra, breakdown of the oxide (Fig. 7) was found to be much more **difficult** to achieve than expected. The implication was that impurities or defects are responsible for breakdowns observed in practical devices, and that an intrinsic limit has not yet been reached. Further work by Wen et al. [44**] investigated BEEM spectroscopy as a function of voltage across the oxide layer. An average image-force dielectric constant was extracted, and a theoretical calculation provided good agreement with this value.

Conclusion

In the 10 years since its inception, a variety of new applications for BEEM have been demonstrated. Recent advances include measurements of band offsets, transport and scattering, confined states, interracial defects, insulating layers, **epitaxial** systems, and strained layers. BEEM methods will continue to provide unique insights into the microscopic nature of interfaces and hot-electron transport.

This paper was produced by the Center for Space Microelectronics Technology, Jet Propulsion Laboratory, California Institute of Technology, and was jointly sponsored by the **Office** of Naval Research and the Ballistic Missile Defense Organization / Innovative Science and Technology **Office** through an agreement with the National Aeronautics and Space Administration (NASA).

References and recommended reading

1. Binnig G, Rohrer H: **Scanning tunneling microscopy**. *Helv Phys Acta* 1982, **55**:726--735.
2. Kaiser WJ, Bell LD: **Direct investigation of subsurface interface electronic structure by ballistic-electron-emission microscopy**. *Phys Rev Lett* 1988, **60**:1406--1409.
3. Bell LD, Kaiser WJ: **Observation of subsurface interface band structure by ballistic electron emission microscopy**, *Phys Rev Lett* 1988, **61**:2368--2371.
4. Bell LD, Kaiser WJ, Hecht MH, Davis LC: **Ballistic electron emission microscopy**. In *Scanning Tunneling Microscopy*. Edited by Stroscio JA, Kaiser WJ. San Diego: Academic Press; 1993:307--348.
5. Prietsch M: **Ballistic-electron-emission microscopy (BEEM): Studies of metal/semiconductor interfaces with nanometer resolution**. *Phys Reports* 1995, **253**:164-233.
6. Bell LD, Kaiser WJ: **Ballistic-electron-emission microscopy: a nanometer-scale probe of interfaces and carrier transport**. *Annu Rev Mater Sci* 1996, **26**:189--222.
7. Hecht MH, Bell LD, Kaiser WJ, Davis LC: **Ballistic hole spectroscopy of interfaces**. *Phys Rev B* 1990,**42**:7663--7666.
8. Hecht MH, Bell LD, Kaiser WJ, Grunthaler FJ: **Ballistic-electron-emission microscopy investigation of Schottky barrier interface formation**, *Appl Phys Lett* 1989, **55**:780--782.
9. Morgan BA, Ring KM, Kavenagh KL, Talin AA, Williams RS, Yasuda T, Yasui T, Segawa Y: **Au/ZnSe contacts characterized by ballistic electron emission microscopy**. *J Appl Phys* 1996, **79**:1532--1535.
10. Coratger R, Ajustron F, Beauvillain J, Dharmadasa IM, Blomfield CJ, Prior KA, Simpson J, Cavenett BC: **Au/n-ZnSe contacts studied with the use of ballistic-electron-emission microscopy**. *Phys Rev B* 1995, **51**:2357--2362.
11. Morgan BA, Ring KM, Kavenagh KL, Talin AA, Williams RS, Yasuda T, Yasui T, Segawa Y: **Role of interface microstructure in rectifying metal/semiconductor contacts: ballistic electron emission microscopy observations correlated to microstructure**. *J Vac Sci Technol B* 1996;**14**:1238--1242.
12. Dharmadasa IM, Blomfield CJ, Coratger R, Ajustron F, Beauvillain J, Simpson J, Prior KA, Cavenett BC: **Microscopic and macroscopic investigation of electrical contacts to n type and p type ZnSe**. *Mater Sci Technol* 1996, **12**:86--89.

13. Coratger R, Girardin C, Beauvillain J, Dharmadasa IM, Samanthilake AP, Frost JEF, Prior KA, Cavenett BC: **Schottky barrier formation at metal/n-ZnSe interfaces and characterization of Au/n-ZnSe by ballistic-electron-emission microscopy.** *J Appl Phys* 1997, **81**:7870--7875.

14. Morgan BA, Talin AA, Bi WG, Kavenagh KL, Williams RS, Tu C, Yasuda T, Yasui T, Segawa Y: **Comparison of Au contacts to Si, GaAs, In_xGa_{1-x}P, and ZnSe measured by ballistic electron emission microscopy.** *Mater Ch Ph* 1996, **46**:224--229.

****15** Siringhaus H, Meyer T, Lee EY, von Kane] H: **Spatial variations of hot-carrier transmission across CoSi₂/Si interfaces on a nanometer scale.** *Phys Rev B* 1996, **53**:15944 -- 15950.

Imaging of variations in interface transmission at the **epitaxial CoSi₂/Si** interface. Enhanced scattering at these defects is observed for **Co Si₂/Si(111)**; for the (100) orientation, a lowering of barrier height on the nanometer scale by these defects is observed.

****16.** Meyer T, von Känel H: **Study of interracial point defects by ballistic-electron-emission microscopy.** *Phys Rev Lett* 1997, **78**:3133--3136.

Study of individual point defects in the **CoSi₂/Si(111)** interface system. First direct evidence that point defects accumulate at dislocation cores.

17. McNabb JW, Craighead HG: **Ballistic electron emission microscopy studies of electron scattering in Au/GaAs Schottky diodes damaged by focused ion beam implantation.** *J Vac Sci Technol B* 1996, **14**:617--622.

18. Sumiya TR, Miura T, Fujinuma H, Tanaka S: **Schottky barrier inhomogeneity at Au/Si(111) interfaces investigated using ultrahigh-vacuum ballistic-electron-emission microscopy.** *Appl Surf Sci* 1997, **117**:329--333.

* 19. Brazel EG, Chin MA, Narayanamurti V, Kapolnek D, Tarsa EJ, DenBaars SP: **Ballistic-electron emission microscopy study of transport in GaN thin films.** *Appl Phys Lett* 1997, **70**:330--332.

Measurements on the **Au/GaN** system. Transmission was observed only in a few areas. Excellent example of BEEM capabilities for the identification of non-ideal interface transport.

***20.** Ventrice Jr CA, LaBella VP, Ramaswamy G, Yu HP, Schowalter LJ: **Measurement of hot-electron scattering processes at Au/Si(100) Schottky interfaces by temperature dependent ballistic electron emission microscopy.** *Phys Rev B* 1996, **53**:3952--3959.

BEEM spectroscopy on **Au/Si(100)** structures at room temperature and at 77K. First observations of the temperature dependence of BEEM current attenuation with Au thickness provided information on the dominant modes of electron scattering.

21. Garcia-Vidal FJ, de Andres PL, Flores F: **Elastic scattering and the lateral resolution of ballistic electron emission microscopy: focusing effects on the Au/Si interface.** *Phys Rev Lett* 1996, **76**:807--810.

****22. Bell LD: Evidence of momentum conservation at a nonepitaxial metal/semiconductor interface using ballistic electron emission microscopy. *Phys Rev Lett* 1996, 77:3893--3896.**
BEEM spectroscopy on Au/Si(111) as a function of Au thickness and temperature. The surprising feature was the appearance of anomalous spectra at 77K for thick Au layers, modeled in terms of parallel momentum conservation at the M/S interface. First identification of multiple passes of electrons through the Au layer from attenuation length measurements.

23. Bell LD: Momentum conservation for hot electrons at the Au/Si(111) interface observed by ballistic-electron-emission microscopy. *J Vac Sci Technol A* 1997, 15:1358--1364.

****24. Guthrie DK, Harrell LE, Henderson GN, First PN, Gaylord TK: Ballistic-electron-emission spectroscopy of Au/Si and Au/GaAs interfaces: Low temperature measurements and ballistic models. *Phys Rev B* 1996, 54:16972--16982.**
Extensive calculations and low-temperature measurements for Au/Si and Au/GaAs, at temperatures down to 7K. The data and modeling also indicated extensive elastic scattering and suggested multiple electron reflections within the metal.

25. Ke ML, Westwood DI, Matthai CC, Richardson BE, Williams RH: Hot-electron transport through Au/GaAs and Au/GaAs/AlAs heterojunction interfaces: ballistic-electron-emission microscopy measurement and Monte Carlo simulation. *Phys Rev B* 1996, 53:4845--4849.

26. Ke ML, Westwood DI, Matthai CC, Richardson BE, Williams RH: Ballistic electron emission microscopy of Au/InAs/GaAs system, *J Vac Sci Technol B* 1996, 14:2786--2789.

****27. O'Shea JJ, Brazel EG, Rubin ME, Bhargava S, Chin MA, Narayanamurti V: Ballistic-electron-emission spectroscopy of $\text{Al}_x\text{Ga}_{1-x}\text{As}/\text{GaAs}$ heterostructures: Conduction band offsets, transport mechanisms, and band structure effects. *Phys. Rev. B* 1997, 56:2026--2035.**
A thorough study of the AlGaAs/GaAs system, Results are presented for the entire Al alloy fraction range. Phonon-assisted intervalley scattering was proposed for certain temperature-dependent contributions to the BEEM spectrum.

***28. Smith DL Kogan SM: Theory of ballistic-electron-emission microscopy of buried semiconductor heterostructures. *Phys Rev B* 1996, 54:10354--10357.**
Theoretical treatment of BEEM spectroscopy through single- and double-barrier semiconductor heterostructures. Calculated transmission coefficients yielded agreement with previously reported BEEM results on double-barrier resonant tunneling structures.

29. Sajoto T, O'Shea JJ, Bhargava S, Leonard D, Chin MA, Narayanamurti V: Direct observation of quasi-bound states and band-structure effects in a double barrier resonant tunneling structure using ballistic electron emission microscopy. *Phys Rev Lett* 1995, 74:3427--3430.

****30 O'Shea JJ Reaves CM, DenBaars SP, Chin MA, Narayanamurti V: Conduction band offsets in ordered GaInP/GaAs heterostructures studied by ballistic-electron-emission microscopy. *Appl Phys Lett* 1996, 69:3022--3024.**

Band-offset measurements on GaInP/GaAs. The offset was observed to decrease with increasing alloy ordering in the GaInP layer. Control over this ordering was demonstrated by growth on disoriented GaAs substrates.

*31. Bhargava S, Blank HR, Narayanamurti V, Kroemer H: **Fermi level pinning position at the Au-InAs interface determined using ballistic-electron emission microscopy.** *Appl Phys Lett* 1997, 70:759--761.

BEEM of Au/InAs/AlSb. Comparison of the measured Au/AlSb band offset with that of InAs/AlSb yielded the Fermi level pinning position in InAs.

**32. Lee EY, Bhargava S, Chin MA, Narayanamurti V, Pond KJ, Luo K: Observation of misfit dislocations at the $\text{In}_x\text{Ga}_{1-x}\text{As}/\text{GaAs}$ interface by ballistic-electron-emission microscopy. *Appl Phys Lett* 1996, 69:940--942.

First imaging of misfit dislocations at the InGaAs/GaAs(100) interface. Surface topographic protrusions resulting from the dislocations were observed in conjunction with diminished BEEM current; a relative displacement of the two features demonstrated that the source was subsurface.

33. Lee EY, Bhargava S, Chin MA, Narayanamurti V: Atomic and **mesoscopic scale characterization of semiconductor interfaces by ballistic electron emission microscopy.** *J Vac Sci Technol A* 1997, 15:1351--1357.

34. Westwood DI, Ke ML, Lelarge F, Laruelle F, Etienne B: **Characterisation of lateral period superlattices by ballistic electron emission microscopy.** *Surf Sci* 1996, 352--354:802--806.

35. Eder C, Smoliner J, Strasser G: **Local barrier heights on quantum wires determined by ballistic-electron-emission microscopy.** *Appl Phys Lett* 1996, 68:2876--2878.

36. Eder C, Smoliner J, Strasser G, Gornik E: **Ballistic-electron-emission microscopy in liquid helium using low-dimensional collector electrodes.** *Appl Phys Lett* 1996, 69:1725--1727.

37. Rubin ME, Medeiros-Ribeiro G, O'Shea JJ, Chin MA, Lee EY, Petroff PM, Narayanamurti V: **Imaging and spectroscopy of single InAs self-assembled quantum dots using BEEM. *Phys Rev Lett* 1996, 77:5268--5271.

BEEM of InAs quantum dots on GaAs. BEEM spectra over the dot areas were observed to differ from spectra away from the dots. Certain spectral structure was attributed to resonant transport through confined states in the quantum dot.

38. Rubin ME, Blank HR, Chin MA, Kroemer H, Narayanamurti V: Local conduction band offset of GaSb self assembled quantum dots on **GaAs.** *Appl Phys Lett* 1997, 70:1590--1592

39. Lee EY, Narayanamurti V, Smith DL: **Monte Carlo simulations of ballistic electron emission microscopy imaging and spectroscopy of buried mesoscopic structures.** *Phys Rev B* 1997, 55:16033--16036.

****40. Kaczer B, Meng A, Pelz JP: Nanometer-scale creation and characterization of trapped charge in SiO₂ films using ballistic electron emission microscopy. *Phys Rev Lett* 1996, 77:91-94.**

BEEM of SiO₂/Si. Suppression of BEEM transmission was observed in areas which had been charged by the STM tip. An increase in BEEM threshold voltage was also observed in these areas.

41. Kaczer B, Pelz JP: Ballistic-electron-emission microscopy studies of charge trapping in SiO₂. *J Vac Sci Technol B* 1996, 14:2864--2871.

42. Ludeke R, Wen HJ: Gate oxide characterization with ballistic-electron-emission microscopy. *Microel Eng* 1997, 36:255--262.

****43. Ludeke R, Wen HJ, Cartier E: Stressing and high-field transport studies on device-grade SiO₂ by ballistic-electron-emission spectroscopy. *J Vac Sci Technol B* 1996, 14:2855 -- 2863.**

BEEM of SiO₂ layers. By comparing Monte Carlo calculations to experimental spectra, breakdown of the oxide was found to be much more **difficult** to achieve than expected. The implication was that impurities or defects, rather than an intrinsic material limit, are responsible for breakdowns observed in devices.

****44. Wen HJ, Ludeke R, News DM, Lo SH: Image force effects and the dielectric response of SiO₂ in electron transport across metal-oxide-semiconductor structures. *J Vac Sci Technol A* 1997, 15:784--789.**

BEEM spectroscopy as a function of voltage across an SiO₂ layer. Theoretical calculations provided good agreement with the extracted image-force dielectric constant.

Figure Captions

Figure]: **Energy diagram** for **BEEM** of a metal/semiconductor **Schottky barrier system**. (a) Tip-sample voltage $V = 0$. (b) Tip-sample voltage $V > V_b$. For this case, some of the injected electrons have **sufficient** energy to enter the semiconductor.

Figure 2: (a) STM image of a 2.8 nm CoSi_2 film. The bright diagonal line is a 0.06 nm protrusion caused by the strain field of a dislocation. Some surface defects, such as (S), are also seen. (b) The BEEM image of this region shows interracial point defects, such as (P), that have been trapped in the core of the dislocation (D). The dislocation displays both empty (E) and occupied (O) regions. From reference 16 (Fig. 1).

Figure 3: Experimental BEEM spectra (circles) obtained for **Au/Si(111)** samples. The solid lines are fits to the data using the Monte Carlo calculations. These calculations include elastic and inelastic scattering, interface and surface reflections, and assume parallel momentum conservation at the metal/semiconductor interface. From reference 24 (Fig. 4).

Figure 4: Simultaneously taken STM and BEEM images of **Au/GaAs/In_{0.2}Ga_{0.8}As/GaAs**. BEEM contrast (-8 pA) is associated directly with the dislocation core, located 50 nm beneath the **epitaxial** surface. The protrusions in the STM image are roughly 1 nm in height and are slightly shifted from the position in the BEEM image. The tip current was 4nA at a tip-sample bias of 1.5V.

Figure 5: Schematic view of BEEM measurements on **SADs**. The dots are grown underneath a thin capping layer so that they are visible in the STM topography. The tip can then be positioned on and off the dot for comparison of transport through the dots with transport through the surrounding material.

Figure 6: Concurrently scanned STM and BEEM images of a single GaSb SAD buried -7.5 nm beneath the Au/ GaAs interface, at 2 nA and -1.6 V. The images clearly show a reduced current through the GaSb dot, consistent with a **local** conduction band offset within the dot.

Figure 7: A successful breakdown sequence for a 3.8 nm oxide stressed with 6 eV (kinetic energy) electrons. The shift to higher threshold between (a) and (b) is due to negative charge at the SiO_2/Si interface. Total injected charge to breakdown is about $6 \times 10^3 \text{ C/cm}^2$. From reference 43 (Fig. 9).

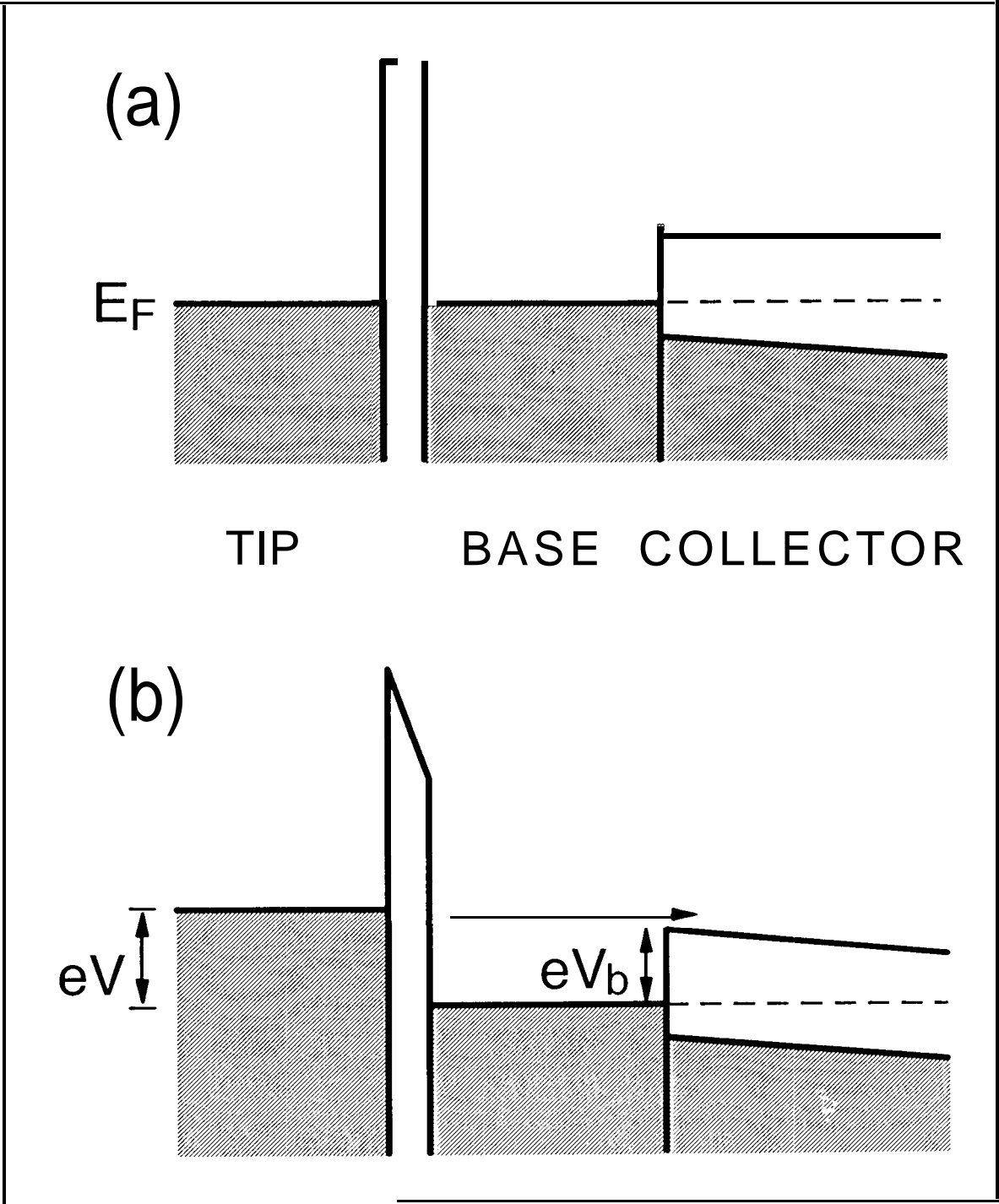


Fig 1

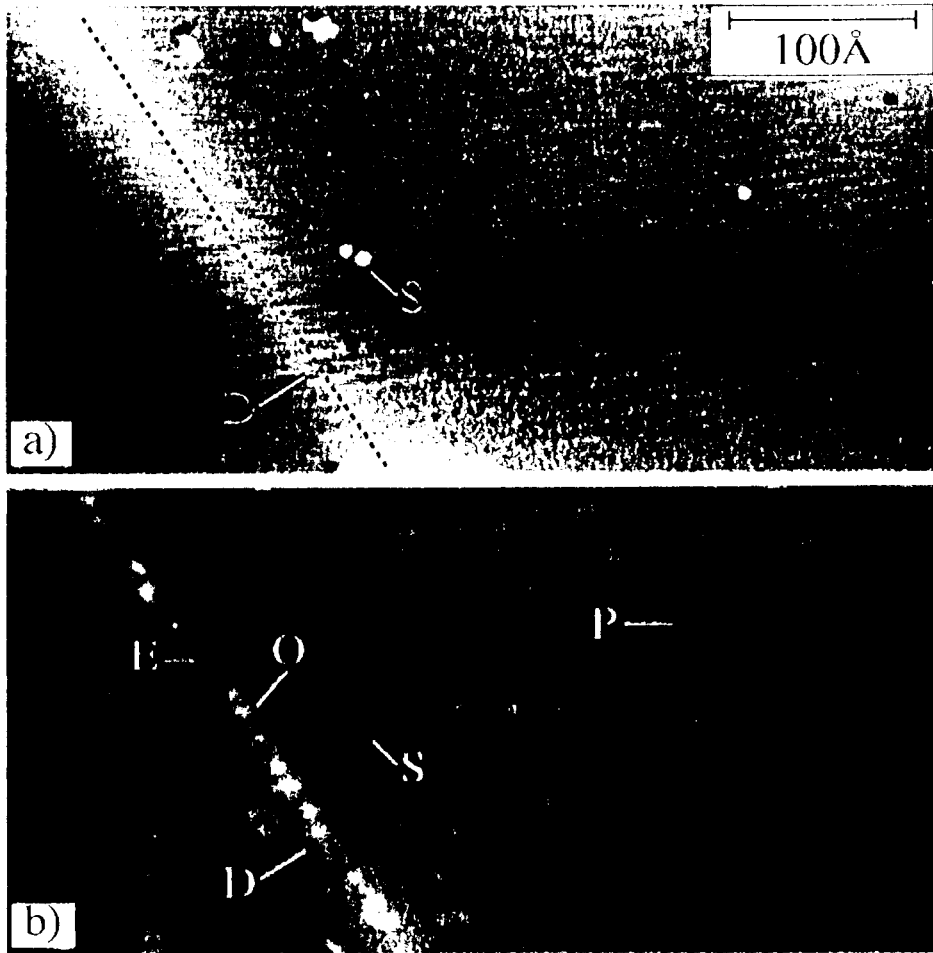


Fig. 1

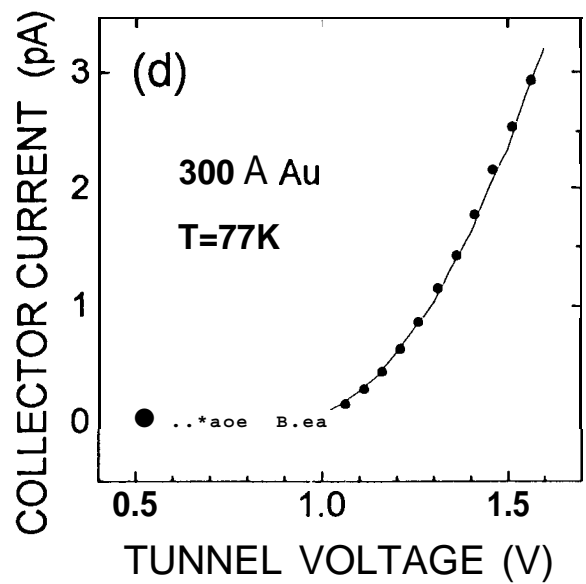
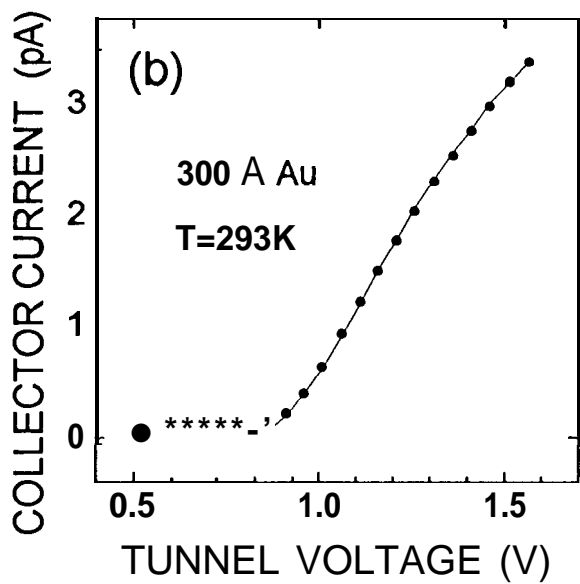
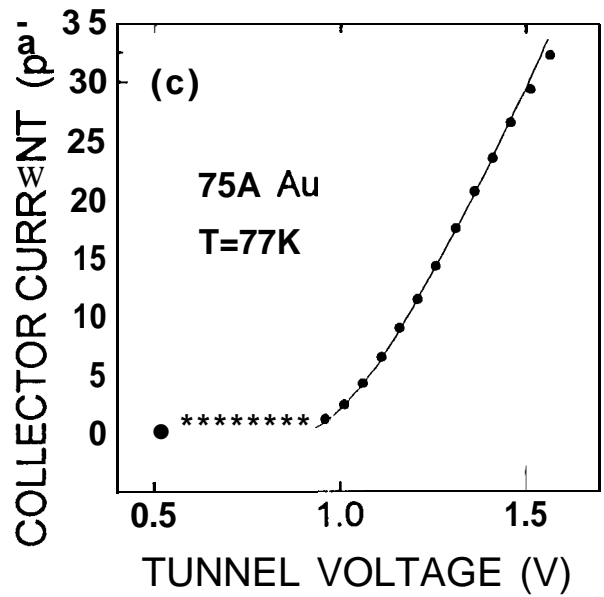
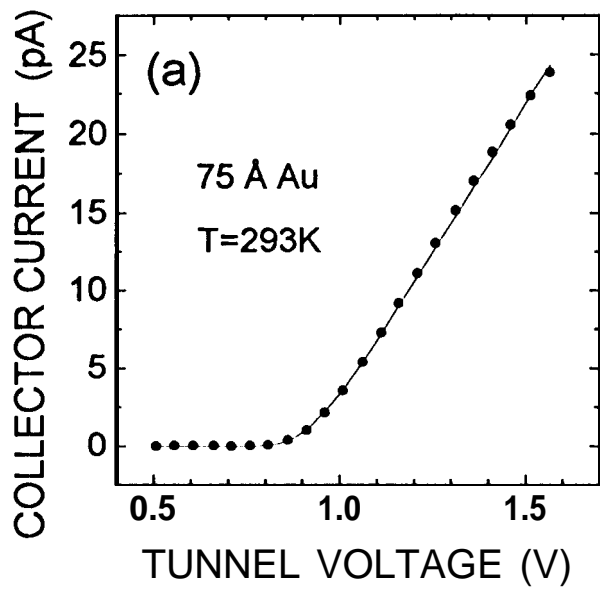
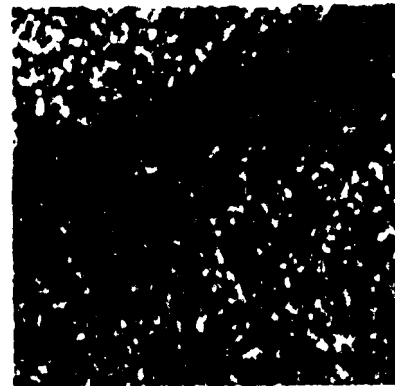
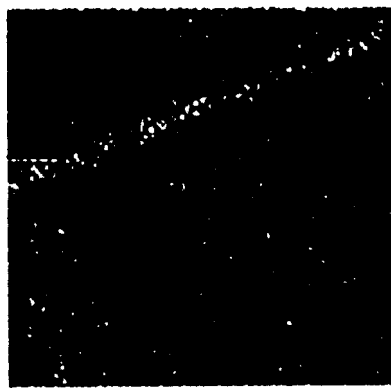


Fig 3

STM

BEEM



400 nm

Fig 4

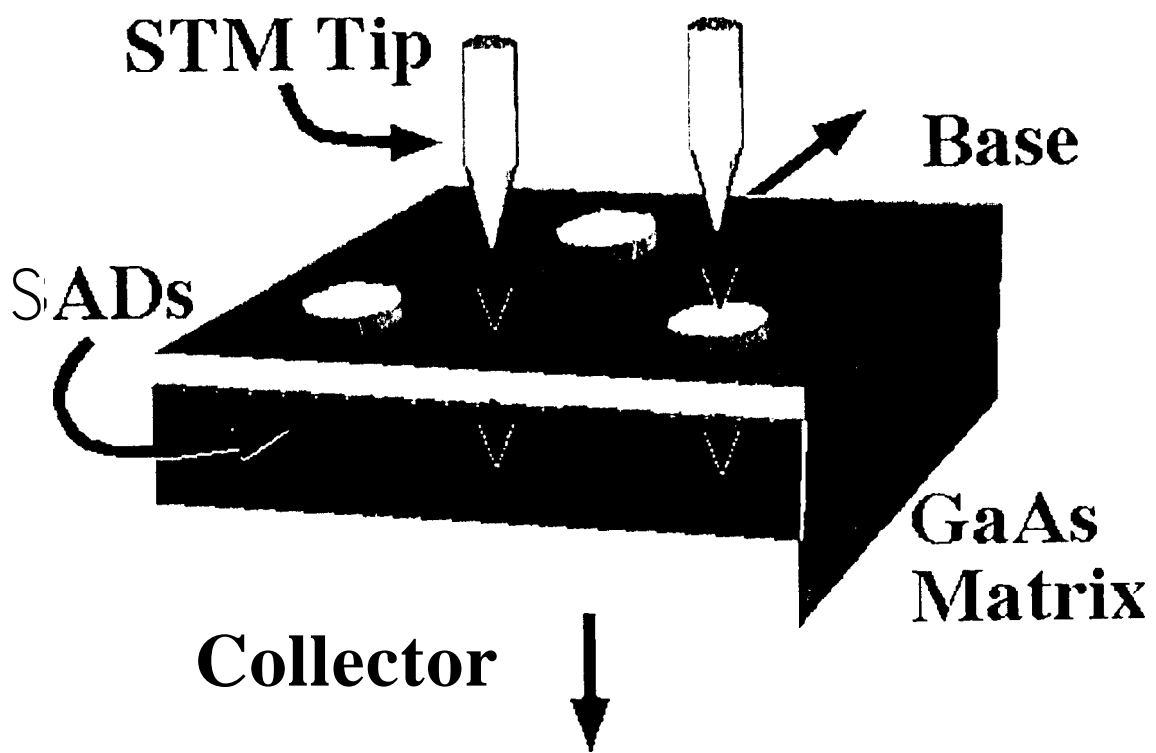


Fig 5

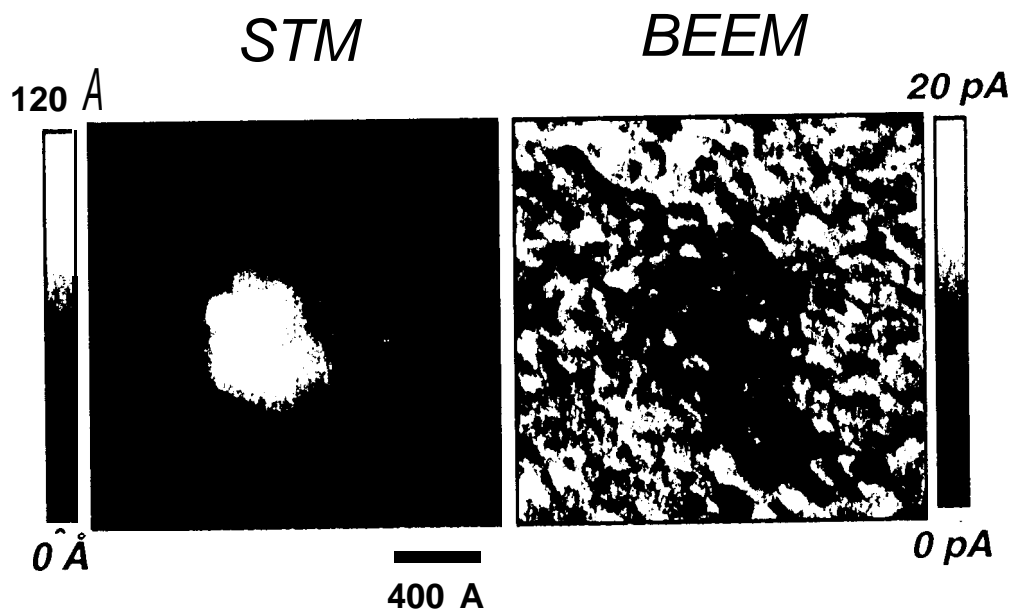


Fig. 6

BEEM for 38 Å SiO₂ stressed at V_T = 1.0 V / I_T = 2 nA

